Molecular Medicine 7(6): 383–392, 2001

Gene Expression in Atherosclerotic Lesion of ApoE Deficient Mice

Dirk Marcus Wuttge,[1] Allan Sirsjö,[1] Per Eriksson,[2] and Sten Stemme[1]

[1]Cardiovascular Research Unit, Center for Molecular Medicine, Department of Medicine, Karolinska Hospital, Stockholm, Sweden

[2]King Gustaf V Research Institute, Department of Medicine, Karolinska Hospital, Stockholm, Sweden

Contributed by H. Wigzell. Accepted February 1, 2001

Abstract

Background: Atherosclerosis, the major cause of mortality and invalidity in industrialized countries, is a multifactorial disease associated with high plasma cholesterol levels and inflammation in the vessel wall. Many different genes have previously been demonstrated in atherosclerosis, although limited numbers of genes are dealt with in each study. In general, data on dynamic gene expression during disease progress is limited and large-scale evaluation of gene expression patterns during atherogenesis could lead to a better understanding of the key events in the pathogenesis of atherosclerosis. We have therefore applied a mouse gene filter array to analyze gene expression in atherosclerotic ApoE-deficient mice.

Materials and Methods: ApoE-deficient mice were fed atherogenic western diet for 10 or 20 weeks and aortas isolated. C57BL/6 mice on normal chow were used as controls. The mRNAs of 15 animals were pooled and hybridized onto commercially available Clontech mouse gene array filters.

Results: The overall gene expression in the ApoE-deficient and control mice correlated well at both time points. Gene expression profiling showed varying patterns including genes up-regulated at 10 or 20 weeks only. At 20 weeks of diet, an increasing number of up-regulated genes were found in ApoE-deficient mice.

Conclusions: The gene expression in atherogenesis is not a linear process with a maximal expression at advanced lesion stage. Instead, several genes demonstrate a dynamic expression pattern with peaks at the intermediate lesions stage. Thus, detailed evaluation of gene expression at several time points should help understanding the development of atherosclerosis and establishment of preventive intervention.

Introduction

Atherosclerosis is the major cause of mortality and invalidity in industrialized countries (1). The disease progresses over several decades and may remain silent until clinical manifestations occur, often with fatal outcome due to, for example, heart infarction or stroke. Although atherosclerosis is a multifactorial disease (1), it is highly correlated with high plasma cholesterol levels (2). Atherosclerosis has been described as an inflammatory disease due to the specific cellular and molecular responses at the site of lesions (2).

The inflammatory changes of the vessel wall recognized today are characterized by early expression of adhesion molecules on activated endothelium (3,4). Blood-derived mononuclear cells, mainly monocytes and T lymphocytes (T cells), extravasate through the endothelial layer (5,6). In the subendothelial space, monocytes differentiate into macrophages and start internalizing modified low-density lipoproteins (6) that have been captured by the extracellular matrix (7). Macrophages may present lipoprotein-derived antigens to T cells (8), that in turn secrete inflammatory cytokines such as interferon-γ (9). In advanced lesions, smooth muscle cells appear in the intima and form a fibrous cap over a necrotic core of the lesion (10).

Mouse models are increasingly used to explore the mechanisms in the pathogenesis of atherosclerosis (11). The ApoE-deficient (ApoE-/-) mouse has gained increasing interest as a suitable model of atherosclerosis and offers the unique possibility to evaluate the disease progress at different stages (12,13).

To increase the understanding of the pathogenesis of the disease, several candidate genes have been explored, although the methodological evaluation has previously been limited to a few genes. The recent development of gene array technology offers new possibilities to evaluate many genes at the same time. The evaluation of the gene expression patterns during the disease progress could lead to a better understanding of the key events in the pathogenesis of atherosclerosis (14).

In this study, we evaluated the gene expression in atherosclerotic ApoE-/- mice at 10 and 20 weeks on western diet applying a commercially available cDNA filter array.

Address correspondence and reprint requests to: Sten Stemme, Cardiovascular Research Unit, Center for Molecular Medicine, L8:03, Karolinska Hospital, S-171 76 Stockholm, Sweden.
Phone: 1 46-8-517 762 23; Fax: 1 46-8-31 31 47;
E-mail: sten.stemme@cmm.ki.se

Materials and Methods

Animals and Tissue Preparation

Female ApoE-/- mice (15) on the B6 background (strain C57BL/6H-Apoe^{TM1UNC129}) were obtained from M&B Breeding and Research Centre

(Bomholtgaard, Denmark) and normal C57BL/6 from Charles River Sverige AB (Uppsala, Sweden) at 6–8 weeks of ages. ApoE-/- mice were fed western diet containing 0.15% cholesterol for 10 or 20 weeks. Mice were sacrificed in groups of five mice by exsanguination under carbon dioxide anesthesia on consecutive days. After perfusion with ice-cold phosphate-buffered saline (PBS), the heart and the total aorta were dissected out and placed on ice-cold PBS. The samples were further rinsed mechanically under the dissection microscope before freezing. The aortas of five mice were pooled and stored at –808C until mRNA preparation. C57BL/6 mice fed normal chow were used as negative controls. Fifteen mice per group were compared.

Histologic Characterization of Atherosclerosis

The hearts were snap-frozen in n-heptane chilled with liquid nitrogen. Frozen cryostat sections were dried, fixed with 4% formaldehyde in PBS at room temperature for 10 min and rinsed in distilled H_2O. After rinse in 60% isopropanol for 2 min, the samples were incubated in 0.67% Oil Red O for 15 min to visualize lipid deposits. Finally, all sections were counterstained with Harris' hematoxylin.

mRNA Isolation, cDNA Synthesis, and Filter Hybridization

The frozen samples were homogenized in a dismembrator (B. Braun, Melsungen AG, Germany). Lysis buffer (Dynal, NY, USA) was added to the homogenate and mRNA isolated on oligo-dT–conjugated magnetic beads (Dynabeads, Dynal). The mRNA quantity was estimated using DNA Dip Stick (Invitrogen, Groningen, The Netherlands). The pooled mRNA from 3 3 5 mice (0.6 μg totally) from each group was precipitated with Na acetate. cDNA was labeled with [α-^{33}P]dATP and hybridized to the mouse gene expression array (Clontech Laboratories Inc., Palo Alto, CA, USA) following the instructions of the manufacturer. The membranes for the two groups of each time were exposed on the same phosphor plate (Fuji BAS 2040, Fujifilm, Tokyo, Japan) for 4–14 hours and were quantified on a BAS 2500 Bio-Imaging Analyzer (Fujifilm).

Real-Time Polymerase Chain Reaction

Twenty nanograms of mRNA from each sample were reverse transcribed (RT) using superscript II according to the manufacturers manual (Gibco, Life technologies, Rockville, MD, USA). One and a half microliters of cDNA was amplified by real-time PCR with 1x TaqMan Buffer, 5mM MgCl2, 200μM of each dNTP, 200μM of each primer, 1.25pM of probe, 0.25U Amp-Erase Uracil N-Glycosylase, 1.25 U AmpliTaq Gold (PE Biosystems, Foster City, CA, USA). For the amplification of the iNOS gene (16), the primers iNOS-FW: 5-CAG CTG GGC TGT ACA AAC CTT-3 and iNOS-RV: 5-CAT TGG AAG TGA AGC GTT TCG-3 (GIBCO/BRL, Grand Island, NY, USA) and probe iNOS-TM: 5-CGG GCA GCC TGT GAG ACC TTT GA-3 (PE Biosystems) were used. For normalization of RNA loading between control samples were run using β-actin (16), the primers β-actin FW: 5-AGA GGG AAA TCG TGC GTG AC-3 and β-actin RW: 5-CAA TAG TGA TGA CCT GGC CGT-3 (GIBCO/BRL, Grand Island, NY, USA) and the probe β-actin TM: 5-CAC TGC CGC ATC CTC TTC CTC CC-3 (PE Biosystems) were used. Each sample was analyzed in duplicates (2 min at 508C, 10 min at 958C, 0.15 min at 958C, and 1 min at 608C) using ABI Prism 7700 Sequence Detector (PE Biosystems). The PCR amplification was correlated against a standard curve. The reactions were performed in MicroAmp Optical 96-Well Reaction Plates (PE Biosystems).

Data and Statistical Analysis

The image was imported in the Image Gauge Version 3.0 computer program (Fujifilm). The light intensity/cm^2 was measured for one gene at a turn, applying exactly equal areas per gene for both groups at each time point. Background values for equal squares were taken at close locations on the filter and subtracted from the raw data. The gene expressions for each group at 10 and 20 weeks of treatment were subjected to regression analysis applying StatView 4.1 software.

Results

Experimental Set-Up

The experimental set-up was designed to analyze the differences between normal arterial walls and atherosclerotic lesions applying a commercially available mouse gene expression array (Clontech) that contained 588 genes. Atherosclerotic ApoE-/- mice were fed atherogenic western diet for 10 and 20 weeks and the gene expression was compared with age-matched C57BL/6 mice on normal chow. Because the lesion size of atherosclerotic plaques is very small in the mouse model, total aortas were dissected out, starting from the beginning of the aortic arch extending to and including the ileac bifurcation, for isolation of mRNA. The root of the aorta was frozen for immunohistologic characterization of the lesions. The extent of atherosclerosis has previously been found to correlate to the disease stages in the aorta (13). Figure 1 shows the extent of atherosclerosis in the root of the aorta in ApoE-/- mice after 10 and 20 weeks of western diet compared to C57BL/6 mice after 20 weeks.

Array Analysis

The quality of the autoradiographic spots was evaluated and only spots with circle-round demarcation from the background were considered positive. Genes that did not meet this criterion in all four groups were considered as not expressed. Following the exclusion of nonexpressed or technically unreadable genes, 370 genes out of 588 genes remained

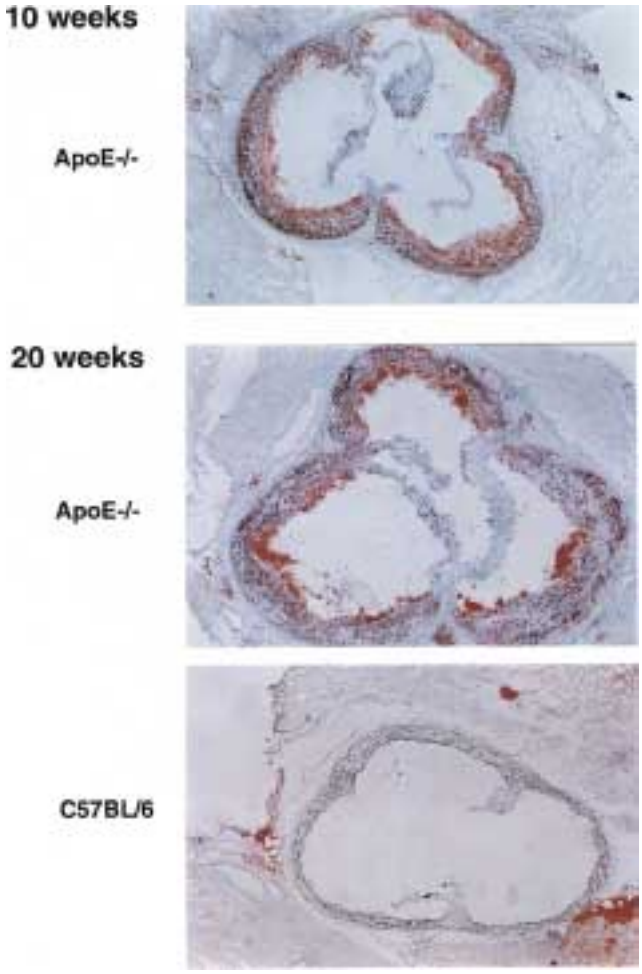

Fig. 1. The histology of the extent of atherosclerosis lesions is shown. The representative roots of the aorta for ApoE-/- mice at 10 and 20 weeks of treatment and a control C57BL/6 mouse at 20 weeks of treatment are depicted. The histologic sections were stained with Oil Red O.

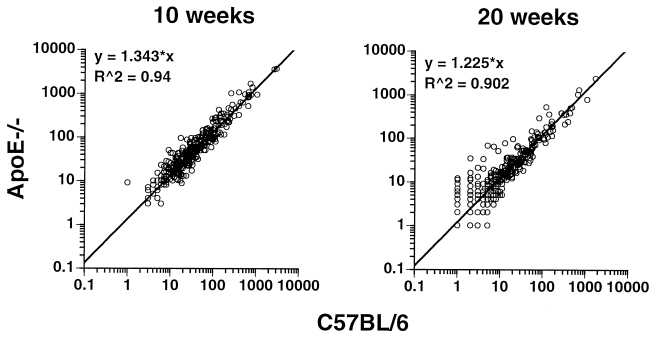

Fig. 2. Regression analysis of the genes expressed in ApoE-/- mice compared to C57BL/6 mice after 10 and 20 weeks of treatment. The scatter diagrams show the expressed genes of ApoE-/- mice versus C57BL/6 mice at 10 (*left*) and 20 weeks (*right*) of treatment and the regression line. The x- and y-axis show the signal intensity. The formula gives the value for the regression line.

for further analysis. To investigate whether the genes expressed in ApoE-/- mice correlated to the expression levels in C57BL/6 mice, intensities of the individual genes expressed in ApoE-/- mice were plotted in a regression analysis against the intensities of the individual genes expressed in C57BL/6 mice for 10 and 20 weeks of treatment (Fig. 2). At the first time point, 10 weeks, the overall gene expressions were highly correlated (R^2 5 .94) between the two groups at an interval of approximately three orders of magnitude and only a few genes visibly deviated from the main trend. At 20 weeks on diet, the correlation coefficient decreased (R^2 5 .902), as would be expected due to the progressive changes in atherosclerotic aortas of ApoE-/- mice, but still showed a high correlation. To normalize the individual genes, first the average gene expression intensities for each group were divided by the average of gene expression intensity of the C57BL/6 mice after 10 weeks of treatment. The expression intensities of the individual genes of the different groups were thereafter divided by the respective normalization factors.

Gene Cluster Analysis

To analyze the gene expression over time, the ratios between ApoE-/- mice and C57BL/6 mice of the included genes at 10 and 20 weeks were calculated. To get a third point for the graphical visualization of the gene expression, the ratios between ApoE-/- and C57BL/6 mice for all genes were set to 1 (5 no difference) for a time point "0 weeks"; assuming that the gene expression of ApoE-/- mice and C57BL/6 mice would correlate even more strongly at the start of the study than after 10 weeks of treatment (Fig. 2), because the disease might not yet have accelerated. To visualize changes in gene expression over time, the web-based program GENECLUSTER (17) was applied; it organizes gene expression into patterns using self-organizing map (SOM) algorithms. A 4 3 2 SOM analysis resulted in eight clusters with different expression patterns (Fig. 3). As expected, a majority of genes showed only small changes in gene expression (Cluster 0, 1, and 2).

Genes summarized in Cluster 3 showed an increased expression in ApoE-/- mice at 10 weeks of diet whereas the gene ratios decreased to 1 or below at 20 weeks (Table 1). The genes from Clusters 4 and 6, showing a strong up-regulation at 20 weeks of diet in the ApoE-/- mice, are summarized in Table 2. Some genes were more than 10-fold up-regulated at that time point.

Genes from Clusters 5 and 7 are summarized in Table 3. These genes showed an increased expression in ApoE-/- mice at both time points, although not as strong at 20 weeks as genes from Clusters 4 and 6.

Quantitative RT-PCR

To validate the pattern and threshold expression levels of genes in the presented analysis we analyzed the

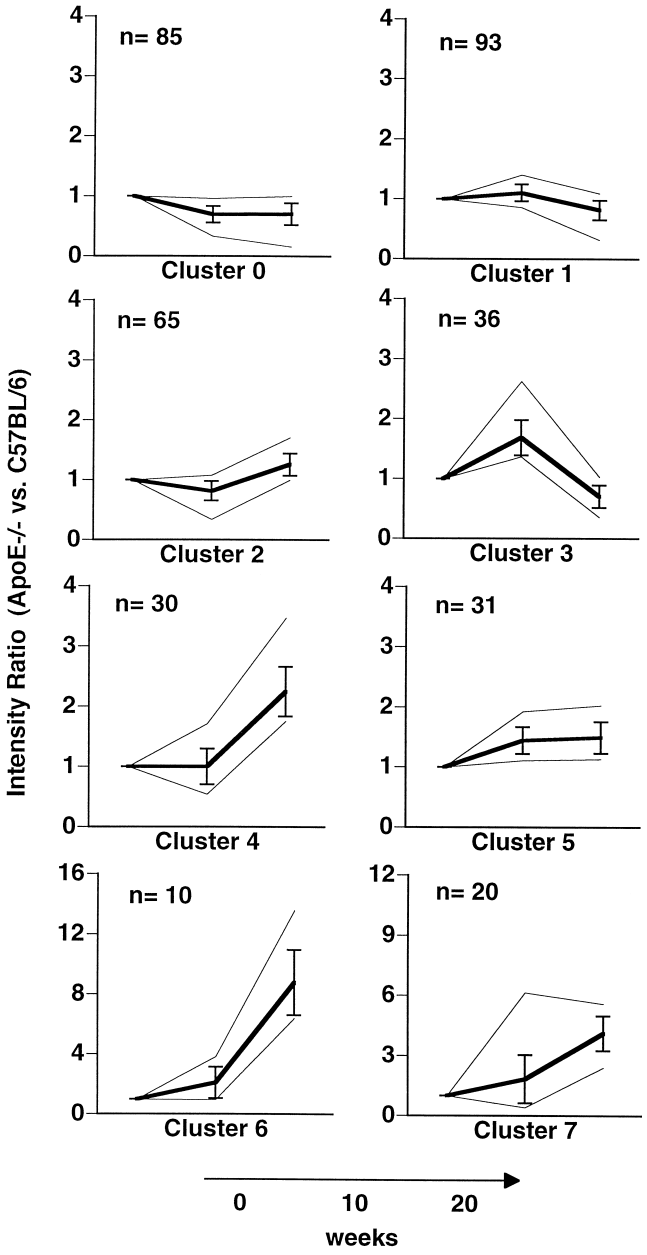

Fig. 3. The gene expression profile during the development of atherosclerosis in ApoE-/- mice is shown in self-organizing maps (SOM). A 4 3 2 SOM summarizes the expression pattern of 370 genes using GENECLUSTER. Genes were submitted as ratios ApoE-/- versus C57BL/6 for 10 and 20 weeks and an imaginary ratio (5 1) as starting point for treatment (see results). The thick line indicates the mean of the ration of the genes in the cluster (*n* 5 number of genes per cluster) and the standard deviation. The thin lines indicate the minimum and maximum values.

expression of inducible nitric oxide sythetase (iNOS, Table 2), a gene with very low intensity in the array analysis, by quantitative real-time RT-PCR. Figure 4 shows RT-PCR values for iNOS. The gene expression of iNOS in the gene array showed a ratio of 0.68 and 2.4 in the ApoE-/- mice at 10 and 20 weeks, respectively. The quantitative RT-PCR showed a 14-fold and 63-fold increase in the ApoE mice at 10 and 20 weeks, respectively.

Discussion

Our study included four groups of 15 animals that gave one analysis point. The high number of animals for each group should acceptably mirror the average gene expression for the different groups, although no statistical evaluation for each time point could be made. It was not feasible to undertake a study including replicates for each point due to the low yield of mRNA. However, regression analysis showed a very strong correlation between ApoE-/- and C57BL/6 gene expression at 10 weeks and a still good correlation for gene expression at 20 weeks. Reproducibility is likely. This suggestion is further supported by studies using commercial filter arrays from Clontech (18). Furthermore, the additional up-regulation of known atherosclerosis-related genes (see below) at 20 weeks compared to 10 weeks supports the reliability of the presented data. The genes that are only increased at 10 weeks of treatment must, however, be interpreted with caution.

To study the detection level of the array, we evaluated the expression of iNOS, a gene that previously has been associated with atherosclerosis (19) and showed low intensity levels in the array analysis. The array analysis and quantitative RT-PCR analysis showed an up-regulation of iNOS at 20 weeks on the diet. However, iNOS values at 10 weeks were lower for ApoE-/- than for C57BL/6 in the array analysis, but showed up-regulation in the quantitative RT-PCR. Thus, the gene array set-up used in this study was less sensitive for the analysis of iNOS expression than quantitative RT-PCR. This might be due to an underestimation of the ApoE-/- values for 10 weeks after normalization toward the average of the intensities of all included genes of the C57BL/6 group at 10 weeks of treatment.

Studies on gene expression of homogenous cell lines in vitro frequently define increases by a factor of 2 as positive up-regulation of gene expression. However, in our system, applying whole aortas to look at changes in gene expression of atherosclerotic tissue, we had to take into account that (i) the aorta of ApoE-/- mice included both diseased tissue as well as unaffected vessel wall, and (ii) that the diseased part in itself consisted of a heterogeneous mixture of different cell types. Thus, the changes we were looking for consisted only of a minute amount of total tissue or mRNA.

Atherosclerosis is a disease involving extravasation of blood-derived cells (5,6). Therefore, the changes of the atherosclerotic vessel wall in ApoE-/- mice should be reflected in the up-regulation of adhesion molecules as well as in novel signs of blood mononuclear cells when compared to nonatherosclerotic C57BL/6 mice. In agreement with this

Table 1. Genes included in Cluster 3

Gene Name	AC no.	10w C57B1/6	10w ApoE-/-	10w Ratio	20w C57B1/6	20w ApoE-/-	20w Ratio
Interleukin-7 receptor	M29697	6	16	2.63	24	9	0.36
Rac1 murine homolog	X57277	24	60	2.48	52	28	0.53
Transducin beta-2 subunit	U34960	30	64	2.15	41	22	0.55
Integrin alpha 5 (CD51)	U14135	19	39	2.05	19	17	0.89
Heat shock 60-kDa protein1 (HSP60); chaperonin; GroEL homolog	X53584	15	29	1.96	30	24	0.80
Golgi 4-transmembrane spanning transporter; MTP	U34259	93	182	1.95	253	135	0.53
Growth hormone receptor	M33324	28	53	1.88	24	16	0.65
Integrin alpha 4	X53176	18	33	1.83	15	12	0.80
Extracellular signal-regulated kinase 1 (ERK1); p44-MAPK; ERT2	M61177	55	99	1.81	78	50	0.64
VLA-3 alpha subunit	D13867	55	97	1.77	76	31	0.41
Ribosomal protein S29	L31609	37	65	1.76	60	48	0.80
CD31; platelet endothelial cell adhesion molecule 1	L06039	106	186	1.76	76	64	0.85
Fyn proto-oncogene;	U70324	10	17	1.71	19	16	0.80
Src family member							
Rab-2 ras-related protein	X95403	113	192	1.70	324	244	0.75
CCHB3; calcium channel beta-3 subunit	U20372	29	49	1.70	26	26	1.00
APC (adenomatous polyposis coli protein)	M88127	14	23	1.68	19	16	0.80
Thrombomodulin	X14432	36	58	1.62	22	17	0.80
IFNgR2; interferon-gamma receptor second (beta) chain	S69336	14	23	1.61	60	54	0.89
Gem induced immediate early protein; Ras family member	U10551	14	23	1.61	24	12	0.51
Insulin receptor	J05149	43	68	1.59	15	16	1.03
SPI3; serpin	U25844	107	169	1.58	91	93	1.03
p58/GTA; galactosyl-transferase associated protein kinase	M58633	7	11	1.57	15	12	0.80
Fibroblast growth factor receptor basic (b FGF-R)	M28998	68	104	1.53	65	35	0.53
Mast cell factor	U44725	14	21	1.52	9	5	0.60
Phospholipase A2	D78647	141	214	1.52	145	119	0.82
Crk adaptor protein	S72408	40	60	1.49	39	38	0.98
Pre-platelet-derived growth factor receptor	X04367	73	108	1.48	67	48	0.72
Glucocorticoid receptor form A	X13358	55	82	1.48	80	69	0.86
Syp; SH-PTP2; adaptor protein tyrosine phosphatase	D84372	56	83	1.48	65	35	0.53
HSP27; heat shock 27-kDa protein 1	U03560	35	50	1.43	108	60	0.56
HMG-14 non histone chromosomal protein	X53476	222	315	1.42	371	264	0.71
Lamimin receptor 1	J02870	137	194	1.41	114	76	0.66
Cdk4; cyclin-dependent kinase 4	L01640	22	31	1.41	19	16	0.80
Androgen receptor	X53779	12	16	1.37	9	3	0.40
Macrophage cannabinoid receptor 2 (CB2)	U21681	4	5	1.37	6	3	0.53
Growth/differentiation factor 2 (GDF-2)	X77113	4	5	1.37	4	2	0.40

Table 2. Genes included in Clusters 4 and 6

Gene Name	AC no.	10w C57B1/6	10w ApoE-/-	10w Ratio	20w C57B1/6	20w ApoE-/-	20w Ratio
CD18 antigen beta subunit; leukocyte adhesion LFA-1	X14951	11	29	2.68	4	59	13.59
Vascular cell adhesion protein 1	M84487	17	65	3.83	11	116	10.72
Nerve growth factor beta (beta-NGF)	K01759	9	18	2.05	2	21	9.60
C5A receptor	L05630	7	7	0.98	2	19	8.80
Cell surface glycoprotein MAC-1 alpha subunit	X07640	7	14	2.05	2	19	8.80
Macrophage inflamatory protein (MIP)	X12531	37	36	0.96	2	19	8.80
CD14 antigen	M34510	15	25	1.69	15	111	7.31
Hepatocyte growth factor; hepapoitein	X72307	9	14	1.52	2	16	7.20
Glutamate receptor channel subunit gamma	X04648	9	34	3.81	9	57	6.60
C-C chemokine receptor; monocyte chemo-attractant protein 1 receptor (MCP-IRA)	U56819	9	13	1.45	4	28	6.40
Interleukin-5 receptor	D90205	5	3	0.55	6	22	3.47
Corticotropin releasing factor receptor	X72305	5	4	0.82	2	7	3.20
Thrombopoietin	L34169	222	149	0.67	2	7	3.20
Gadd45; growth arrest and DNA-damage-inducible protein	L28177	26	19	0.74	6	16	2.40
Gut-specific Kruppel-like factor GKLF	U20344	19	21	1.08	6	16	2.40
Inducible nitric oxide synthase (iNOS)	M87039	15	10	0.64	4	10	2.40
Endothelin b receptor (Ednrb)	U32329	10	10	0.96	4	10	2.40
DNA-binding protein SMBP2	L10075	3	2	0.68	2	5	2.40
Glutamate receptor; ionotropic NMDA2A (epsilon 1)	D10217	14	8	0.54	2	5	2.40
Bone Morphogenetic protein 8a (BMP-8a)	M97017	11	10	0.87	2	5	2.40
Macrophage inflamatory protein 2 alpha (MIP2-alpha)	X53798	6	9	1.48	2	5	2.40
Interleukin 15	U14332	8	14	1.71	2	5	2.40
Ablphilin-1 (abi-1); similar to HOXD3	U17698	23	23	0.98	15	33	2.17
c-Fes proto-oncogene	X12616	12	10	0.87	13	28	2.13
Interferon alpha-beta receptor	M89641	8	7	0.86	6	14	2.13
Neuronal-cadherin (N-cadherin)	M31131	19	17	0.90	6	14	2.13
Keratinocyte growth factor FGF-7	Z22703	17	21	1.25	6	14	2.13
Nuclear factor related to P45 NF-E2	U20532	96	152	1.58	119	250	2.11
Clusterin; complement lysis inhibitor	L08235	275	379	1.38	305	615	2.02
PKC-beta; protein kinase C beta-II type	X53532	6	7	1.14	4	9	2.00
CD 40L receptor (TNF receptor family)	M83312	7	8	1.17	4	9	2.00
CD3 antigen delta polypeptide	M33158	8	8	1.03	4	9	2.00
Integrin alpha 2 (CD49b)	X75427	5	5	0.96	4	9	2.00
Glutathione peroxidase (plasma protein); selenoprotein	U13705	75	84	1.11	30	60	2.00
Insulin-like growth factor-IA	X04480	74	94	1.27	54	107	1.98
Bax; Bcl-2 heterodimerization partner and homolog	L22472	51	47	0.93	32	62	1.92
Ezrin; NF-2 (merlin) related filament/plasma membrane associated protein	X60671	9	11	1.22	13	24	1.87
SRY-box containing gene 4	X70298	40	25	0.62	9	16	1.80
Urokinase type plasminogen activator	X02389	15	16	1.10	9	16	1.80
FAF1; Fas-associated protein factor	U39643	151	129	0.86	11	19	1.76

Table 3. Genes included in Cluster 5 and 7

Gene Name	AC no.	10w C57B1/6	10w ApoE-/-	10w Ratio	20w C57B1/6	20w ApoE-/-	20w Ratio
G-CSF receptor	M58288	5	7	1.37	2	12	5.60
Monotype chemoattractant protein 3	S71251	54	74	1.37	6	36	5.60
Nuk tyrosine-protein kinase receptor	L25890	14	10	0.73	2	10	4.80
Cellular retinoic acid binding protein II	M35523	5	10	2.05	4	21	4.80
Gamma interferon induced monokine	M34815	10	29	2.95	2	10	4.80
Cathepsin L	X06086	132	288	2.18	28	131	4.68
CD44 antigen	M27129	35	52	1.49	19	86	4.44
Vav proto-oncogene	X64361	23	24	1.04	4	19	4.40
Ung1; uracil-DNA glycosylase	X99018	17	7	0.40	4	19	4.40
P-selectin	X91144	42	35	0.83	4	19	4.40
Integrin alpha 6	X69902	8	15	1.88	4	19	4.40
Syk tyrosine-protein kinase	U25685	8	19	2.40	9	35	4.00
Ikaros DNA binding protein	L03547	7	10	1.47	2	9	4.00
c-Fms proto-oncogene	X68932	42	48	1.15	43	164	3.80
Cathepsin D	x53337	390	734	1.88	259	907	3.50
Intercellular adhesion molecule-1	X52264	13	20	1.53	4	14	3.20
Macrophage inflammatory protein 1 beta	M35590	3	4	1.37	2	7	3.20
Interleukin 1 beta	M15131	3	5	1.60	2	7	3.20
Cathepsin B	M14222	255	697	2.73	177	504	2.85
SLAP	U29056	1	6	6.16	2	5	2.40
Transforming growth factor beta	M13177	67	106	1.58	56	114	2.03
cAMP-dependent protein kinase type I-beta regulatory chain	M20473	4	7	1.71	4	9	2.00
Erf; Ets-related transcription factor	U58533	28	54	1.93	32	62	1.92
Pim-1 proto-oncogene	M13945	13	19	1.46	17	31	1.80
MDR1; P-glycoprotein	M14757	13	16	1.21	9	16	1.80
uPAR1 (CD87)	X62700	9	12	1.37	9	16	1.80
DP-1 (DRTF-polipeptide 1) cell cycle regulatory transcription factor	X72310	28	48	1.71	30	54	1.77
Kinesin-like protein KIF 3B	D26077	23	30	1.31	13	22	1.73
B7-2 (CD86); CD28 antigen antigen Iigand 2	L25606	8	11	1.37	11	17	1.60
CD28 (receptor for B71)	M34563	8	9	1.11	4	7	1.60
Platelet-derived growth factor (A chain)	M29464	19	23	1.19	13	21	1.60
Interleukin 6	X51975	14	18	1.27	6	10	1.60
Membrane-type matrix matalloproteinase	X83536	68	86	1.27	37	59	1.60
Interleukin-converting enzyme (ICE)	L28095	203	226	1.11	153	238	1.55
Elf-1 (Ets family transcription factor)	U19617	16	29	1.84	19	29	1.51
Cathepsin H	U06119	171	236	1.38	114	166	1.45
Fli-1 ets-related proto-oncogene	X59421	14	17	1.25	17	24	1.40
I-κB (I-kappa B) alpha chain	U36277	29	45	1.56	22	29	1.36
Insulin-like growth factor binding protein-4 (IGFBP-4)	X81582	67	101	1.50	164	218	1.33
CACCC Box- binding protein BKLF	U36340	33	38	1.16	69	90	1.30
Stat1	U06924	36	58	1.62	45	59	1.29
Interferon-inducible protein 1	U19119	13	23	1.79	28	36	1.29
Interferon-gamma receptor	M28233	11	15	1.37	11	14	1.28
Basic domain/leucine zipper transcription factor	L36435	4	7	1.71	15	19	1.26
GapIII; GTPase-activating protein	U20238	16	19	1.20	19	24	1.24
Beta-actin	M12481	721	1156	1.60	1443	1777	1.23
T-lymphocyte activated protein	M31042	65	85	1.31	41	50	1.22
MEK protein kinase	L02526	29	37	1.28	65	78	1.20
Transcription factor LRG-21	U19118	23	34	1.46	9	10	1.20
Interleukin-6 receptor beta chain	M83336	148	242	1.63	162	190	1.17
Glutathione S-transferase (microsomal)	J03752	49	70	1.43	37	41	1.13

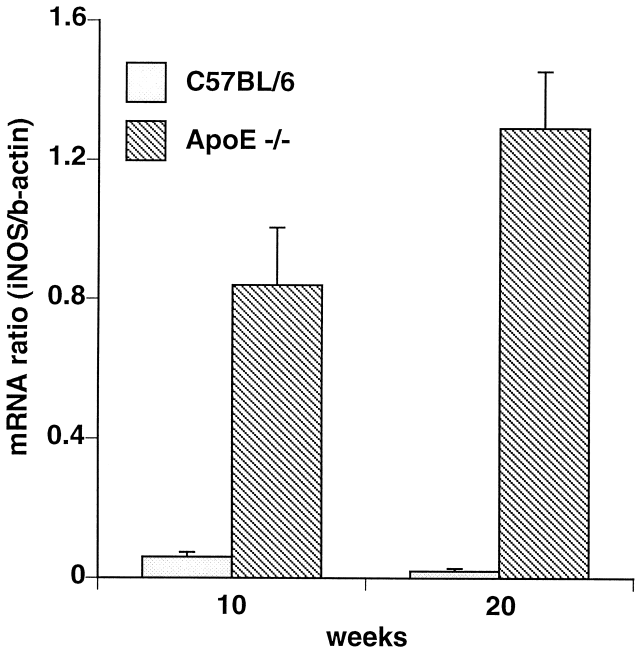

Fig. 4. Quantitative RT-PCR of for iNOS, a gene with low expression values in the gene array. The evaluation of the expression levels for iNOS by quantitative RT-PCR is shown for all groups. The y-axis indicates the mRNA ratio of iNOS divided by the mRNA of β-actin. Mean ± SEM of three pooled samples each containing five mice for each time point.

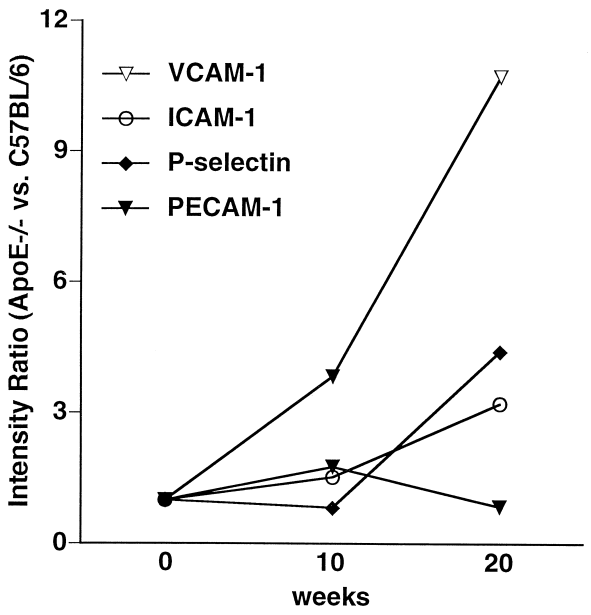

Fig 5. Expression pattern of adhesion molecules during the development of atherosclerosis in ApoE-/- mice are shown. The changes of expression for four adhesion molecules are depicted in the diagram. The y-axis indicates the ratios of gene expression between ApoE-/- mice and C57BL/6 control mice for 10 and 20 weeks of diet.

hypothesis, VCAM-1 (4) was up-regulated 3.83-fold in ApoE-/- mice at 10 weeks, and further increased to an 10.72-fold induction at 20 weeks compared to C57BL/6 mice. A similar pattern showed ICAM-1 (20) that increased from a 1.52-fold induction at 10 weeks to a 3.20-fold up-regulation at 20 weeks. A graphical illustration of the expression pattern of adhesion molecules present in Tables 1 through 3 is shown in Figure 5.

Mac-1, a marker for macrophages, showed an expression level that increased from a 2.05-fold induction at 10 weeks, to an 8.8-fold induction at 20 weeks paralleling the increased influx of macrophages into the subendothelial space at sites of atherosclerosis. Additionally, CD14 and CD18, which are both expressed in monocytes/ macrophages, increased from a 1.69- and 2.68-fold induction at 10 weeks to a 7.31- and 13.59-fold up-regulation at 20 weeks of treatment. Interestingly, the c-Fms proto-oncogene, encoding for the receptor of the macrophage colony-stimulating factor, which previously has been demonstrated to be up-regulated in human atherosclerotic lesions (21), showed a 1.15-fold induction at 10 weeks that increased to 3.8-fold at 20 weeks. CD3, a marker for T cells, showed a 1.03-fold induction at 10 weeks and increased to a ratio of 2.00 at 20 weeks. Similarly, CD4 was up-regulated 1.1-fold (7.5 versus 7.0) at 10 weeks and 1.3-fold (8.6 versus 6.5) at 20 weeks (Cluster 2) in ApoE-/- mice compared to C57BL/6 mice. Additionally, CD40 that has evolved as an important signaling path in atherosclerosis (22), increased from a 1.14-fold induction to a 2.00-fold increase in ApoE-/- mice at 20 weeks of treatment.

Moreover, the increased expression of platelet-derived growth factor (1.19- and 1.60-fold induction at 10 and 20 weeks, respectively) might be associated with an increased proliferation and migration of smooth muscle cells from the media into the intima, a key feature of atherosclerosis (23,24). The expression of transcription factor egr-1 (Cluster 2) was increased at 20 weeks of treatment, although at a rather low level (a ratio of 0.99 and 1.3 at 10 and 20 weeks, respectively, when comparing the egr-1 expression in ApoE-/- and C57BL/6 mice). Egr-1 has recently been detected in human atherosclerotic lesions and confirmed in a related mouse model, the LDL receptor-deficient mouse (25). Phospholipase AII is expressed in our study in normal C57BL/6 mice and at increased levels in atherosclerotic ApoE-/- mice at 10 weeks (Table 1). These results are similar to the previous findings of the expression of phospholipase AII in normal and atherosclerotic human vascular tissue (26). Together, this indicates that ratios down to 1.13 might be interpreted as an up-regulation in our study.

In the present study, we compared ApoE-/- mice on a high cholesterol diet with C57BL/6 on normal diet to analyze the differences between atherosclerotic lesions and nonatherosclerotic vessels. We cannot exclude that some effects of gene expression may be due to compounds of the western diet (increased

cholesterol levels), which are not due to development of atherosclerosis per se. However, the increases in expression of many genes associated with atherosclerosis over time imply that our experimental set-up truly mirrors atherosclerosis-related gene expression.

In addition to the established atherosclerosis-associated genes, several new candidate genes were found up-regulated in ApoE-/- mice. The macrophage chemoattractant protein-3 (MCP-3) (Table 3), a chemokine that attracts both macrophages and T cells, has previously been shown to be induced in vascular smooth muscle cells after cytokine stimulation (27). MCP-3 binds to the chemokine CC receptors-2 (CCR-2), similar to the related MCP-1, and CCR-3 (28). Interestingly, MCP-3 has additionally been suggested as an inhibitor of inflammation after cleavage by gelatinase 4 (29). Nerve growth factor (NGF) is up-regulated at 10 weeks and further increased at 20 weeks of treatment (Table 2). NGF is expressed in vascular smooth muscle in vascular remodeling after injury (30,31), but has not yet been evaluated in the context of atherosclerosis. Interestingly, extensive studies indicate that NGF might have an important role in inflammation (32–34). NGF and bFGF have been shown to increase mRNA levels of cathepsin-S, -B, and –L (35). These proteases were up-regulated during atherosclerosis in the present study and were confirmed by immunohistochemistry in the lesions (Jormsjö S et al, manuscript submitted). $CD4^{1}$ T cells and mast cells might be a potential source for NGF in the atherosclerotic lesions (36,37). Hepatocyte growth factor (Table 2) has previously been shown to be present in rat and human vascular endothelial and smooth muscle cells (38). Hepatocyte growth factor has been shown to increase the expression of CD44 in endothelial cells and might thus contribute to adherence and extravasation of inflammatory cells (39,40). The overall expressions of both nerve growth factor and hepatocyte growth factor are low in C57BL/6, indicating that the up-regulation might be specific for the aortas of the ApoE-/- mice. Cellular retinoic acid binding protein-II (CRABP-II), a gene that is regulated by the retinoic acid receptor (RAR) signaling path (41), showed an increased expression and supports the previous finding of RAR-mediated signaling in human atherosclerosis (42). The low overall expression suggests a rather low retinoic acid mediated signaling in the control tissue (Table 3).

In conclusion, we studied gene expression during the development of atherosclerosis in the commonly used ApoE-/- mouse applying the commercially available Clontech mouse gene array. Having the drawbacks of our study design in mind, the gene expression in our study reflected features in the development of atherosclerosis that have been described earlier by others. Furthermore, the results indicate that gene expression is not a linear process with a maximal expression at advanced lesion stage. Rather, the pathogenesis should already to be evaluated in detail at early time points, to understand the development of atherosclerosis and to establish a preventive intervention. The present analysis is based on the evaluation of 377 genes and it will be necessary to interpret the present results in conjunction with future studies to evaluate the significance of the different findings.

Acknowledgments

We are greatly in debt to Inger Bodin for technical assistance. This project was supported by grants from the Swedish Medical Research Council (12660), the Swedish Heart-Lung Foundation, the Torsten and Ragnar Söderberg Foundation, the Åke Wiberg Foundation, the Magnus Bergvall Foundation, the Foundation for Old Servants, and the Professor Nanna Svartz Foundation.

References

1. Braunwald E. (1997) Shattuck lecture-cardiovascular medicine at the turn of the millennium: triumphs, concerns, and opportunities. *N. Engl. J. Med.* **337:** 1360–1369.
2. Ross R. (1999) Atherosclerosis-an inflammatory disease. *N. Engl. J. Med.* **340:** 115–126.
3. Dong ZM, Chapman SM, Brown AA, Frenette PS, Hynes RO, Wagner DD. (1998) The combined role of P- and E-selectins in atherosclerosis. *J. Clin. Invest.* **102:** 145–152.
4. Cybulsky MI, Gimbrone MJ. (1991) Endothelial expression of a mononuclear leukocyte adhesion molecule during atherogenesis. *Science* **251:** 788–791.
5. Hansson GK, Seifert PS, Olsson G, Bondjers G. (1991) Immunohistochemical detection of macrophages and T lymphocytes in atherosclerotic lesions of cholesterol-fed rabbits. *Arterioscler. Thromb.* **11:** 745–750.
6. Gerrity RG. (1981) The role of the monocyte in atherogenesis: I. Transition of blood-borne monocytes into foam cells in fatty lesions. *Am. J. Pathol.* **103:** 181–190.
7. Hurt E, Camejo G. (1987) Effect of arterial proteoglycans on the interaction of LDL with human monocyte-derived macrophages. *Atherosclerosis* **67:** 115–126.
8. Stemme S, Faber B, Holm J, Wiklund O, Witztum JL, Hansson GK. (1995) T lymphocytes from human atherosclerotic plaques recognize oxidized low density lipoprotein. *Proc. Natl. Acad. Sci. U.S.A.* **92:** 3893–3897.
9. Hansson GK, Holm J, Jonasson L. (1989) Detection of activated T lymphocytes in the human atherosclerotic plaque. *Am. J. Pathol.* **135:** 169–175.
10. Newby AC, Zaltsman AB. (1999) Fibrous cap formation or destruction—the critical importance of vascular smooth muscle cell proliferation, migration and matrix formation. *Cardiovasc. Res.* **41:** 345–360.
11. Lichtman AH, Cybulsky M, Luscinskas FW. (1996) Immunology of atherosclerosis: the promise of mouse models. *Am. J. Pathol.* **149:** 351–357.
12. Breslow JL. (1996) Mouse models of atherosclerosis. *Science* **272:** 685–688.
13. Nakashima Y, Plump AS, Raines EW, Breslow JL, Ross R. (1994) ApoE-deficient mice develop lesions of all phases of atherosclerosis throughout the arterial tree. *Arterioscler. Thromb.* **14:** 133–140.
14. Hiltunen MO, Niemi M, Yla-Herttuala S. (1999) Functional genomics and DNA array techniques in atherosclerosis research. *Curr. Opin. Lipidol.* **10:** 515–519.

15. Piedrahita JA, Zhang SH, Hagaman JR, Oliver PM, Maeda N. (1992) Generation of mice carrying a mutant apolipoprotein E gene inactivated by gene targeting in embryonic stem cells. *Proc. Natl. Acad. Sci. U.S.A.* **89:** 4471–4475.
16. Overbergh L, Valckx D, Waer M, Mathieu C. (1999) Quantification of murine cytokine mRNAs using real time quantitative reverse transcriptase PCR. *Cytokine* **11:** 305–312.
17. Tamayo P, Slonim D, Mesirov J, et al. (1999) Interpreting patterns of gene expression with self-organizing maps: methods and application to hematopoietic differentiation. *Proc. Natl. Acad. Sci. U.S.A.* **96:** 2907–2912.
18. Smid-Koopman E, Blok LJ, Chadha-Ajwani S, Helmerhorst TJ, Brinkmann AO, Huikeshoven FJ. (2000) Gene expression profiles of human endometrial cancer samples using a cDNA-expression array technique: assessment of an analysis method. *Br. J. Cancer* **83:** 246–251.
19. Detmers PA, Hernandez M, Mudgett J, et al. (2000) Deficiency in inducible nitric oxide synthase results in reduced atherosclerosis in apolipoprotein E-deficient mice. *J. Immunol.* **165:** 3430–3435.
20. Nakashima Y, Raines EW, Plump AS, Breslow JL, Ross R. (1998) Upregulation of VCAM-1 and ICAM-1 at atherosclerosis-prone sites on the endothelium in the ApoE-deficient mouse. *Arterioscler. Thromb. Vasc. Biol.* **18:** 842–851.
21. Salomon RN, Underwood R, Doyle MV, Wang A, Libby P. (1992) Increased apolipoprotein E and c-fms gene expression without elevated interleukin 1 or 6 mRNA levels indicates selective activation of macrophage functions in advanced human atheroma. *Proc. Natl. Acad. Sci. U.S.A.* **89:** 2814–2818.
22. Mach F, Schonbeck U, Libby P. (1998) CD40 signaling in vascular cells: a key role in atherosclerosis? *Atherosclerosis* **137**(suppl):S89–S95.
23. Wilcox JN, Smith KM, Williams LT, Schwartz SM, Gordon D. (1988) Platelet-derived growth factor mRNA detection in human atherosclerotic plaques by in situ hybridization. *J. Clin. Invest.* **82:** 1134–1143.
24. Murry CE, Bartosek T, Giachelli CM, Alpers CE, Schwartz SM. (1996) Platelet-derived growth factor-A mRNA expression in fetal, normal adult, and atherosclerotic human aortas. Analysis by competitive polymerase chain reaction. *Circulation* **93:** 1095–1106.
25. McCaffrey TA, Fu C, Du B, et al. (2000) High-level expression of Egr-1 and Egr-1-inducible genes in mouse and human atherosclerosis. *J. Clin. Invest.* **105:** 653–662.
26. Hurt-Camejo E, Andersen S, Standal R, et al. (1997) Localization of nonpancreatic secretory phospholipase A2 in normal and atherosclerotic arteries. Activity of the isolated enzyme on low-density lipoproteins. *Arterioscler. Thromb. Vasc. Biol.* **17:** 300–309.
27. Wang X, Li X, Yue TL, Ohlstein EH. (2000) Expression of monocyte chemotactic protein-3 mRNA in rat vascular smooth muscle cells and in carotid artery after balloon angioplasty. *Biochim. Biophys. Acta* **1500:** 41–48.
28. Kunkel SL. (1999) Through the looking glass: the diverse in vivo activities of chemokines [comment]. *J. Clin. Invest.* **104:** 1333–1334.
29. McQuibban GA, Gong JH, Tam EM, McCulloch CA, Clark-Lewis I, Overall CM. (2000) Inflammation dampened by gelatinase A cleavage of monocyte chemoattractant protein-3. *Science* **289:** 1202–1206.
30. Horiba M, Kadomatsu K, Nakamura E, et al. (2000) Neointima formation in a restenosis model is suppressed in midkine-deficient mice. *J. Clin. Invest.* **105:** 489–495.
31. Nemoto K, Fukamachi K, Nemoto F, et al. (1998) Gene expression of neurotrophins and their receptors in cultured rat vascular smooth muscle cells. *Biochem. Biophys. Res. Commun.* **245:** 284–288.
32. Aloe L, Skaper SD, Leon A, Levi-Montalcini R. (1994) Nerve growth factor and autoimmune diseases. *Autoimmunity* **19:** 141–150.
33. Sanico AM, Stanisz AM, Gleeson TD, et al. (2000) Nerve growth factor expression and release in allergic inflammatory disease of the upper airways. *Am. J. Respir. Crit. Care Med.* **161:** 1631–1635.
34. Braun A, Appel E, Baruch R, et al. (1998) Role of nerve growth factor in a mouse model of allergic airway inflammation and asthma. *Eur. J. Immunol.* **28:** 3240–3251.
35. Liuzzo JP, Petanceska SS, Devi LA. (1999) Neurotrophic factors regulate cathepsin S in macrophages and microglia: a role in the degradation of myelin basic protein and amyloid beta peptide. *Mol. Med.* **5**:334–343.
36. Lambiase A, Bracci-Laudiero L, Bonini S, et al. (1997) Human CD41 T cell clones produce and release nerve growth factor and express high-affinity nerve growth factor receptors. *J. Allergy Clin. Immunol.* **100:** 408–414.
37. Leon A, Buriani A, Dal Toso R, et al. (1994) Mast cells synthesize, store, and release nerve growth factor. *Proc. Natl. Acad. Sci. U.S.A.* **91:** 3739–3743.
38. Nakamura Y, Morishita R, Higaki J, et al. (1995) Expression of local hepatocyte growth factor system in vascular tissues. *Biochem. Biophys. Res. Commun.* **215:** 483–488.
39. Hiscox S, Jiang WG. (1997) Regulation of endothelial CD44 expression and endothelium-tumour cell interactions by hepatocyte growth factor/scatter factor. *Biochem. Biophys. Res. Commun.* **233:** 1–5.
40. Adams DH, Harvath L, Bottaro DP, et al. (1994) Hepatocyte growth factor and macrophage inflammatory protein 1 beta: structurally distinct cytokines that induce rapid cytoskeletal changes and subset-preferential migration in T cells. *Proc. Natl. Acad. Sci. U.S.A.* **91:** 7144–7148.
41. Niforas P, Chu MD, Bird P. (1996) A retinoic acid/cAMP-responsive enhancer containing a cAMP responsive element is required for the activation of the mouse thrombomodulin-encoding gene in differentiating F9 cells. *Gene* **176:** 139–147.
42. Wuttge DM, Rommert A, Eriksson U, et al. Induction of CD36 by all-trans Retinoic Acid. Retinoic Acid Receptor Signaling in the Pathogenesis of Atherosclerosis. *FASEB J* 2001 March 20 [epub ahead of print]